



# International Journal of Engineering Researches and Management Studies

## EVALUATION AND PHOTOCATALYTIC DEGRADATION OF POLYAROMATIC HYDROCARBONS IN PETROLEUM REFINERY WASTEWATER

Sawsan A. Mahmoud<sup>\*1</sup>, Omayma E. Ahmed<sup>1</sup>, A. M. Mousa<sup>2</sup>, Nabila A. Ali<sup>3</sup>

<sup>\*1</sup>Egyptian Petroleum Research Institute, Nasr City, Cairo, Egypt

<sup>2</sup>Chemistry Departments, Faculty of science, Ain Shams

<sup>3</sup>Suez Oil Processing Company, Suez, Egypt.

### ABSTRACT

Due to the importance of Gulf area, the present study was performed in discharge basin around the Coastal area of petroleum Suez Company, which is located in the northwest of the Gulf. In our previous work, Sediment samples were collected from five stations at different distances along discharge basin of the company and the concentrations of Poly-aromatic Hydrocarbons (PAHs) were determined in sediment samples. At all of the stations, the concentration of ΣPAHs was higher than the guideline value (**4022ng g<sup>-1</sup>**). The concentration of PAHs in the sediments ranged between 22333.983 up to 73597.864ng g<sup>-1</sup>.

In this work, different wt. % of Copper/TiO<sub>2</sub> was prepared by wet impregnation method. The prepared materials were studied by nitrogen adsorption-desorption isotherm, X-ray diffraction, FTIR and Raman spectroscopy and high resolution transmission electron microscopy. The prepared materials were used to remove the Polyaromatic Hydrocarbons of the discharge basin of petroleum Suez Company by photocatalysis technique using batch reactor equipped with UV-vis solar light. Our results showed that the 0.09wt. % Cu/TiO<sub>2</sub> has a higher photocatalytic activity in the photocatalytic degradation than 0.04wt. %. The polyaromatic hydrocarbons in water were successfully removed after 240 min of irradiation

**Keywords-** discharge basin, petroleum Suez Company, PAHs, guideline value, photocatalysis, TiO<sub>2</sub>, copper phthalocyanine

### I. INTRODUCTION

Oil pollution of aquatic ecosystems is a serious problem in many parts of the world. The released oil undergoes several weathering processes (biotic and abiotic) that alter its physical and chemical composition [1,2]. The main weathering processes that contribute to the fate of oil in aquatic ecosystems include evaporation, spreading, dissolution, dispersion, emulsification, photodegradation, biodegradation and sedimentation. Although evaporation and cleanup activities may reduce the amount of oil released into the water, a fraction of this oil dissolves in seawater and continues to exert adverse effects on the marine environment [3]. It has been established that the dissolved rather than the emulsified or the absorbed fraction of the oil that is acutely toxic to marine life. The traditional treatment of refinery wastewater is based on the physicochemical and mechanical methods and further biological treatment in the integrated activated sludge treatment unit. With respect to the fact that different concentrations of aliphatic and aromatic petroleum hydrocarbons are present in the wastewater, among which the aromatic fraction is not readily degraded by the conventional treatments and is more toxic, there is still a need for advanced techniques to remove this sort of pollutants as much as possible.

Several solutions are proposed in this regard; including use of coagulants [4,5], coagulation enhanced by centrifugation [6], ultra filtration [7,8] or sorption on organo-minerals [9]; with a level of advantage for each of them.

Photodegradation may play distinctly important roles in oil breakdown in the marine environment. Biodegradation may be slow in tropical and subtropical latitudes when nutrients are limited. On the other hand, Photodegradation may be of greater importance in environments with intense solar radiation such as those in Egypt. Photo-oxidation may most likely enhance the dispersion of the oil spills by transforming the oil components into more water-soluble oxygenated ones. This process may also be responsible for changes in physical properties of the exposed oil [10, 11].



## International Journal of Engineering Researches and Management Studies

The photocatalysis is one of the techniques, which are so-called “advanced oxidation processes (AOPs)”. These processes can completely degrade the organic pollutants into harmless substances such as  $\text{CO}_2$  and  $\text{H}_2\text{O}$  under moderate conditions. The AOPs are characterized by the production of  $\text{OH}\cdot$  radicals which are extraordinary reactive species and capable of mineralizing organic pollutants [12]. They are also characterized by a little selectivity of attack, which is a useful attribute for an oxidant used in wastewater treatment. They attack most of the organic molecules with different rates; therefore, providing a valuable technique when multi-contaminated wastewater, e.g. refinery wastewater is considered. The photocatalysis has been tested on many different compounds including environmentally relevant organic compounds and in many different processes [13-15].

Due to the large band gap such as band gap of  $\text{TiO}_2$  (anatase: 3.2 eV; rutile: 3.0 eV), many semiconductors ordinarily used can generate electron-hole pair only when illuminated by ultraviolet light, which is a limit to the photo-electronic transition efficiency of solar photocatalysis because the portion of UV-light in the solar spectrum is only about 3–5% of total sunlight [16,17]. Therefore, the development of visible-light-driven photocatalysts is indispensable. In this study, we intend to apply a photocatalysis technology for refinery wastewater treatment through simple synthesis and characterization of photoactive material. To make adequate use of solar energy in decontaminating water [18-20].

## II. METHODOLOGY

### Area of study

Laboratory treatment was performed using the sediment of discharge basin of Suez Oil Processing Company, which is located in the northwest of the Gulf. Sediment sample was collected from station of the discharge basin of the company. The oil was extracted and concentrated to approximately 0.2 ml using dry nitrogen. The oil content in sediment was then calculated after removing the solvent till constant wt. and the concentrations of Poly-aromatic Hydrocarbons (PAHs) were determined in sediment samples using High Performance liquid chromatography. The concentration of  $\Sigma$ PAHs was higher than the guideline value ( $4022 \text{ ng g}^{-1}$ ) due to the aromatic outlet to discharge basin of petroleum Suez Company [21]. The extracted oil was weighed and dissolved in a small volume of methanol and then diluted with distilled water to a known volume to carry out the photocatalytic degradation process.

### Catalyst preparation

Pure  $\text{TiO}_2$  and Cu / $\text{TiO}_2$  in different wt. % 0.04 and 0.09 were prepared by sol-gel method at ambient pressure and temperature as follows;  $\text{TiO}_2$  was prepared by dissolving titanium isopropoxide in isopropanol. Ammonia solution was added dropwise with constant stirring to adjust pH at 9. The precipitate was then centrifuged and dried at  $120^\circ \text{C}$  then calcined at  $500^\circ \text{C}$  for 2 hours. Doping  $\text{TiO}_2$  with copper phthalocyanine was carried out as follows:

A calculated weight of solid  $\text{TiO}_2$  was stirred overnight in known concentration of copper phthalocyanine in a solution containing poly (diallyldimethylammonium chloride) conductive polymer. The powder was filtered, dried at  $120^\circ \text{C}$  and calcined at  $250^\circ \text{C}$  for 2 hours.

### Catalyst characterization

Nitrogen adsorption/desorption isotherms of the synthesized samples were measured on ASAP2010, at  $-196^\circ \text{C}$  after degassing at  $200^\circ \text{C}$  for 4 h. X-ray diffraction patterns were recorded with a Pan Analytical Model X' Pert Pro, which was equipped with  $\text{CuK}\alpha$  radiation ( $\lambda = 0.1542 \text{ nm}$ ). High Resolution Transmission electron microscopy (HRTEM) analysis was carried out using a JEOL JEM-1230 electron microscope operating at 120 kV. Raman spectra were collected using a Renishaw Via 2000 system with an argon ion laser emitting at 100 and 800 nm. FT-IR spectra of the samples were carried out using ATI unicam (Mattson 936) Bench Top spectrometer.



## International Journal of Engineering Researches and Management Studies

### *Photocatalytic degradation of polyaromatic hydrocarbons extract*

Experiments were carried out in vertical reactor, resemble to the published previous work [22] with capacity of about 500 ml (Figure 1). The UV-Vis lamp with the highest irradiation peak at 365 nm was immersed in a silica jacket which allows the circulation of water to remove any thermal effect due to the irradiation. The silica jacket was placed in a jar containing polluted water. For well-mixing of the catalyst and polluted water a magnetic stirrer was used. At different irradiation time intervals, samples of the irradiated water were withdrawn for the analysis using HPLC (PerkenElmr series 200) equipped with photo-diode-array detector and at  $\lambda = 245$  nm and Brownlee Analytical PAHs  $5 \mu\text{m}$  (250 $\times$ 4.6 mm) column. The mobile phase was acetonitrile / water with a gradient elution in which a change in the ratio of acetonitrile to water from 60/40 to 100% within 15 min was used at flow rate of  $1.2 \text{ ml min}^{-1}$ .

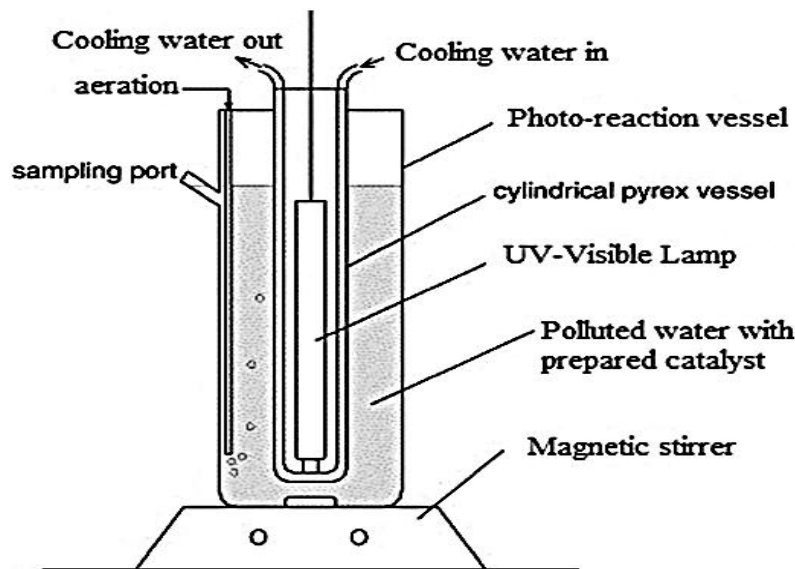


Figure 1: Schematic diagram of photo-reactor

### III. RESULTS & DISCUSSION

#### **N<sub>2</sub> adsorption desorption isotherm**

The prepared samples display Type IV isotherm according to the IUPAC classification, which are typical for mesoporous solids [23] (Figure 2A&B). In Table 1 the surface and structural properties of pure TiO<sub>2</sub> and different wt. % Cu/TiO<sub>2</sub> are summarized. From BET results, it is clear that the presence of polymer leads to a certain stabilization of the surface area. The BET surface area, the pore volume and pore size have not change significantly with increasing the Cu loading.



# International Journal of Engineering Researches and Management Studies

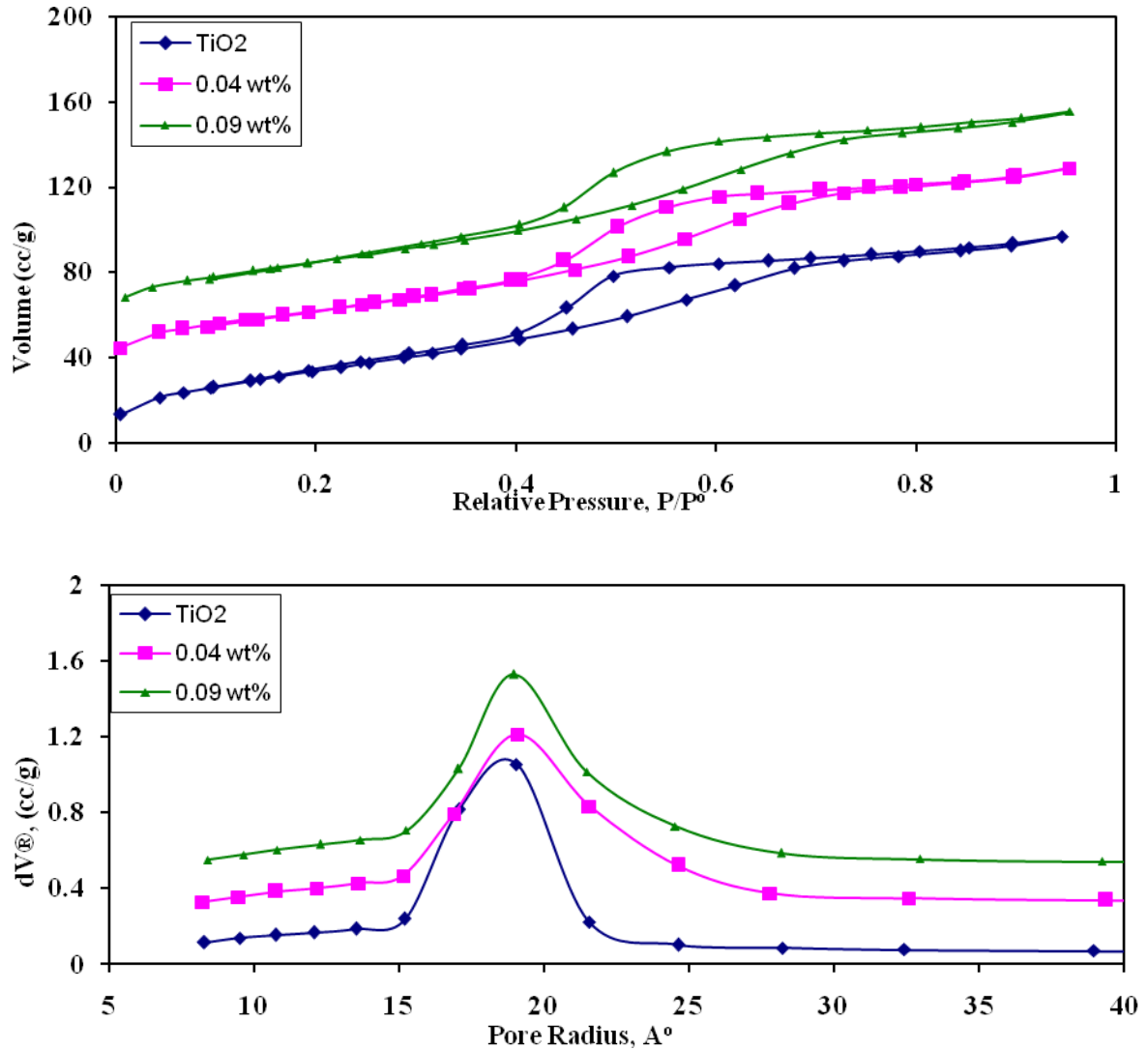


Figure 2:  $N_2$  adsorption-desorption isotherm of  $TiO_2$ , 0.04 and 0.09 wt.%  $Cu/TiO_2$  (A) and the corresponding pore size distribution (B).



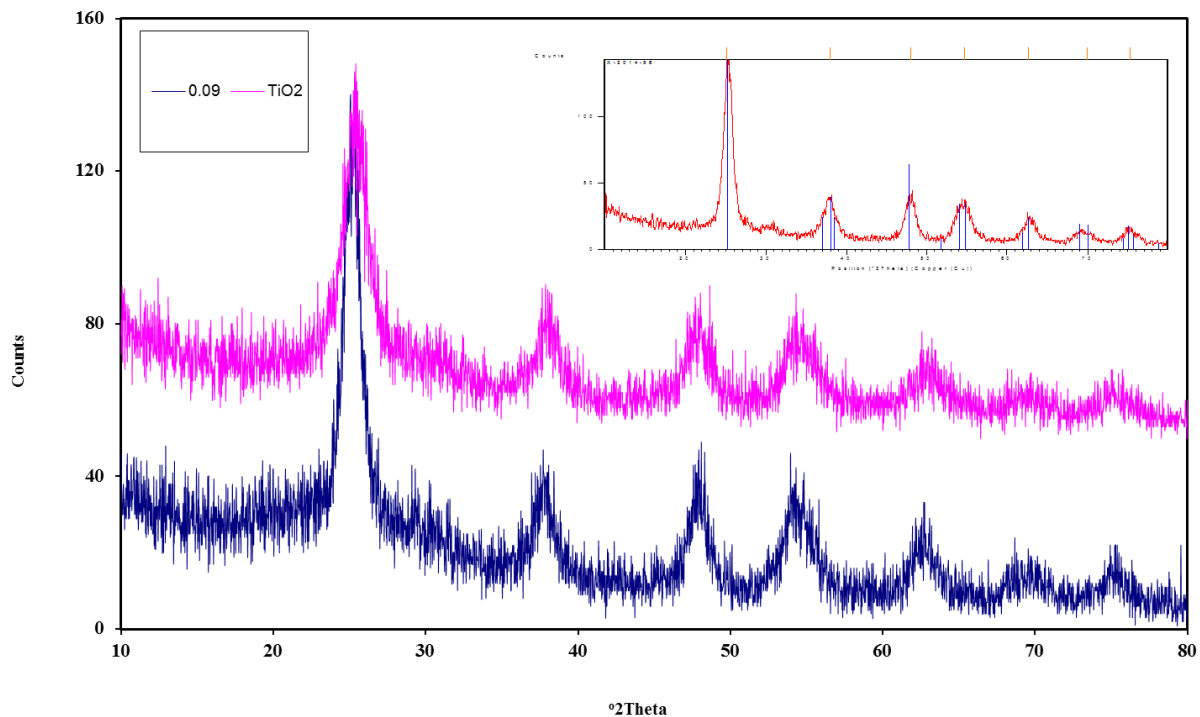
## International Journal of Engineering Researches and Management Studies

*Table 1: Surface properties and crystallite size of TiO<sub>2</sub>, 0.04 wt.% Cu/TiO<sub>2</sub> and 0.09 wt.% Cu/TiO<sub>2</sub>*

| catalyst                      | BET Surface area, m <sup>2</sup> /g | Average Pore radius, nm | Total Pore volume, cc/g | Crystallite size, nm |
|-------------------------------|-------------------------------------|-------------------------|-------------------------|----------------------|
| TiO <sub>2</sub>              | 131.8                               | 2.30                    | 0.15                    | 3.2                  |
| 0.04 wt.% Cu/TiO <sub>2</sub> | 121.9                               | 2.51                    | 0.15                    | 2.86                 |
| 0.09 wt.% Cu/TiO <sub>2</sub> | 132.0                               | 2.44                    | 0.16                    | 1.66                 |

### X-ray diffraction

Figure 3 shows the XRD of bare TiO<sub>2</sub> and Cu/TiO<sub>2</sub> in different wt. %. The diffraction peaks observed at the 2θ values of 25.42, 38.68, 48.15, and 74.4 correspond to the anatase phase of TiO<sub>2</sub> and were assigned to the (101), (004), (200), and (215) crystallographic planes, respectively. No characteristic peaks for copper were found in the XRD. This indicates that, copper is highly dispersed on the TiO<sub>2</sub> surface. A decrease in intensity of the (101) peak and increase in the broadness with increasing in the concentration of copper. This is due to the presence of polymer which suppresses the increase in size of the crystal. Due to the large atomic radius of Cu<sup>+2</sup> (1.57 Å) compared to Ti<sup>4+</sup> (0.68 Å), it is impossible for Cu ions to act as interstitial ions in the TiO<sub>2</sub> matrix. Hence Cu<sup>2+</sup> ions may only replace Ti<sup>4+</sup> in the lattice sites. Table 1 shows the calculated crystallite size using Scherrer's equation. The results show that the crystallite size was 3.2 nm, 2.86 nm and 1.66 nm for bare TiO<sub>2</sub>, 0.04 and 0.09 wt. % Cu/TiO<sub>2</sub>, respectively.



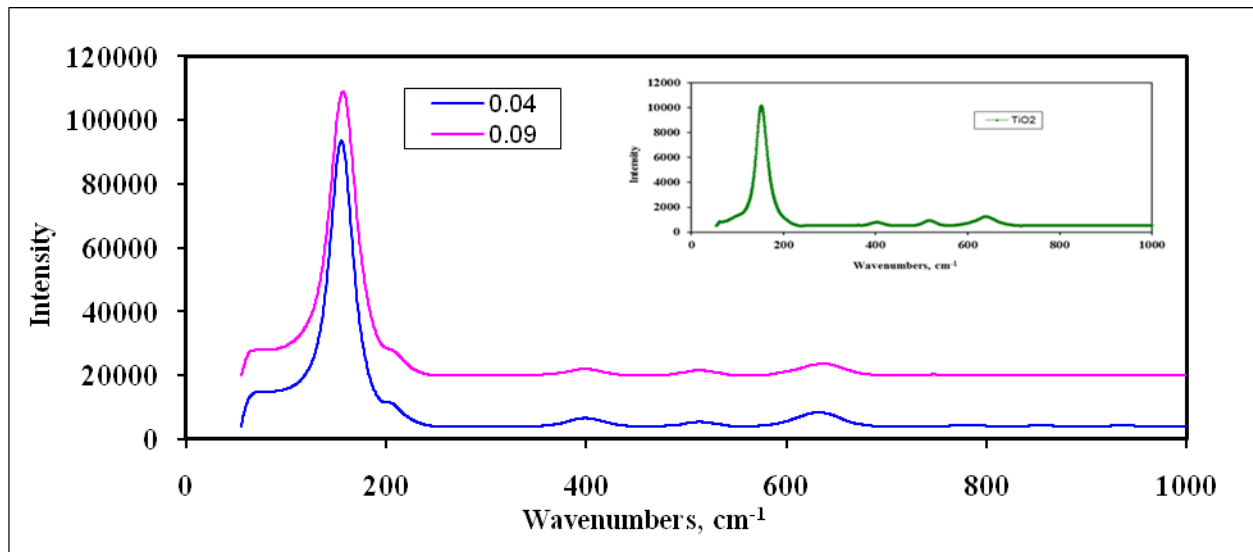
### Raman spectroscopy

Figure 4 shows the Raman spectroscopy in the range of 100–1000 cm<sup>-1</sup>. The anatase TiO<sub>2</sub> phase was observed at 156 (E<sub>g</sub>), 428 (B<sub>1g</sub>), 533 (A<sub>1g</sub>), and 659 cm<sup>-1</sup> (E<sub>g</sub>). The inset at the top of Figure 4 shows blue shift in the lowest frequency (E<sub>g</sub>) mode upon impregnation with copper. No signals corresponding to copper particles were identified in the



## International Journal of Engineering Researches and Management Studies

samples. This may be attributed to the relatively low concentration of copper loaded onto the  $\text{TiO}_2$  and its weak Raman scattering. The peak intensities were decreased by the copper loading, this indicates that the interaction between copper and  $\text{TiO}_2$  affected the Raman resonance of the  $\text{TiO}_2$  [24] without phase transition due to the change in the electronic structure of  $\text{TiO}_2$  with scandium doping [25].



*Figur4: Raman spectroscopy of  $\text{TiO}_2$ , 0.04 and 0.09 wt. %  $\text{Cu/TiO}_2$*

### FTIR spectroscopy

Figure 5 shows the FTIR of the prepared samples. The bare  $\text{TiO}_2$  display the presence of absorption bands at  $594 \text{ cm}^{-1}$  due to the presence of stretching vibration of Ti-O-Ti. A band at  $1400 \text{ cm}^{-1}$  could be attributed to N-O asymmetric stretching bond. A vibrational band at  $1636 \text{ cm}^{-1}$  could be assigned to O-H bending of hydroxyl group. The broad band at  $3418 \text{ cm}^{-1}$  is due to stretching mode of surface hydroxyl group. The same groups appear in 0.04wt.% and 0.09wt.%  $\text{Cu/TiO}_2$ .

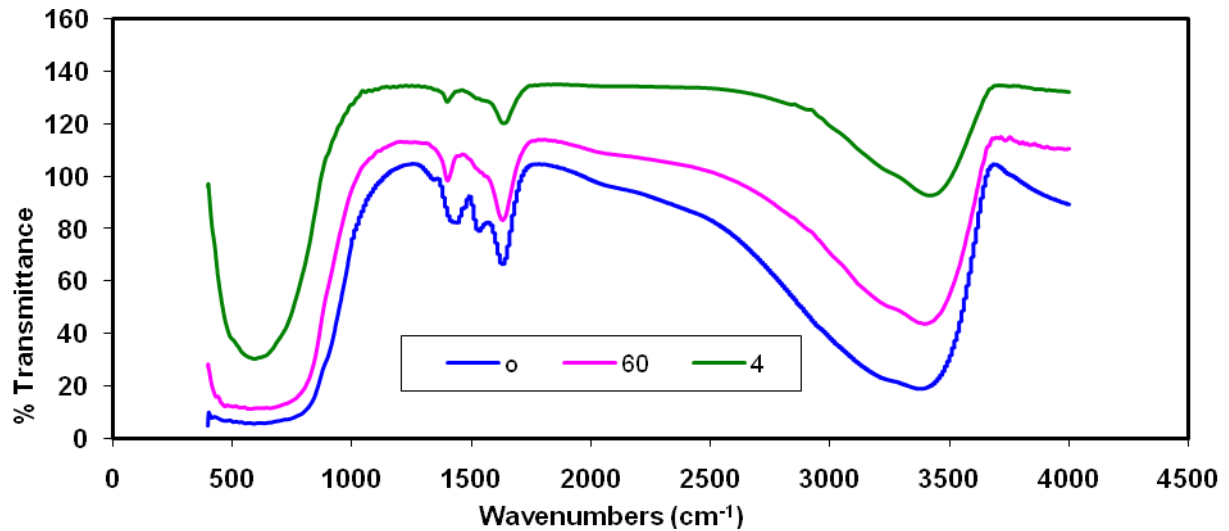
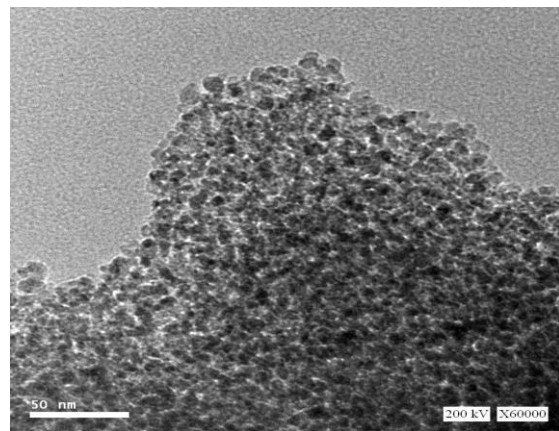
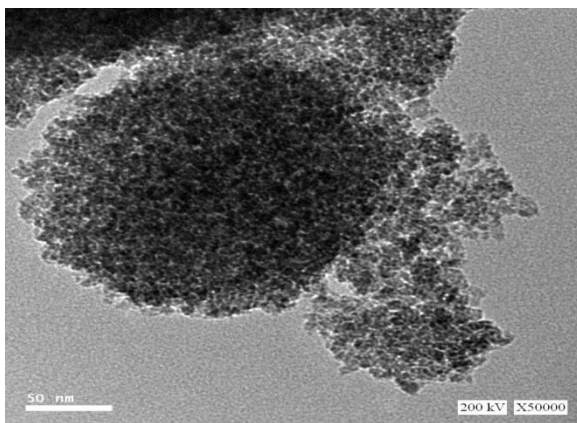


Figure 5: FTIR of  $\text{TiO}_2$ , 0.04wt.%  $\text{Cu/TiO}_2$  and 0.09wt.%  $\text{Cu/TiO}_2$

**High Resolution transmission electron microscopy (HRTEM)**

Figure 6 (A-C) shows the HRTEM of  $\text{TiO}_2$ , 0.04wt.% and 0.09wt.%. The Figure shows the change in crystallite size according to the copper doping. The samples display a cubic morphology with different sizes; in case of  $\text{TiO}_2$  the particle size was 3.2 nm. The particle size decrease as the copper loading increases.



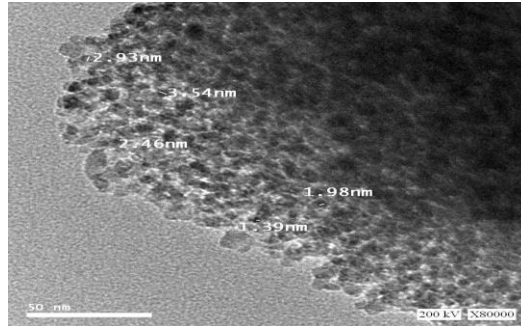


Figure 6: HRTEM of  $TiO_2$ (A), 0.04 wt.% Cu/ $TiO_2$  (B) and 0.09 Wt.% Cu/ $TiO_2$ (C)

#### Photocatalytic degradation:

The photocatalytic experiments were carried out using extracted oil from sediment of Suez company drainage. The sample under study represents the outlet of Suez oil Petroleum company at <50m/west. Figure 7 shows the map of stations along the drainage basin of Suez Oil Petroleum Company (SOPC). The sample was extracted and diluted with distilled water. The extracted oil from different stations of the Company contains 2-3 rings and 4-rings, beside 5-6-ring [21], the PAHs in sediment were Acenaphthylene (A), Acenaphthene (Ace), Fluorene (F), phenanthrene (Phe), anthracene (Ant), Fluoranthene (Flu), pyrene (Py), benzo(a)anthracene (BaA), benzo(b)fluoranthene (BbF), Benzo[a] Pyrene (BAP), indeno[1,2,3-] pyrene. Figure 8 shows the chemical structure of PAHs in this study. Table 2 shows the concentrations of PAHs in the sample under consideration as indicated by HPLC.

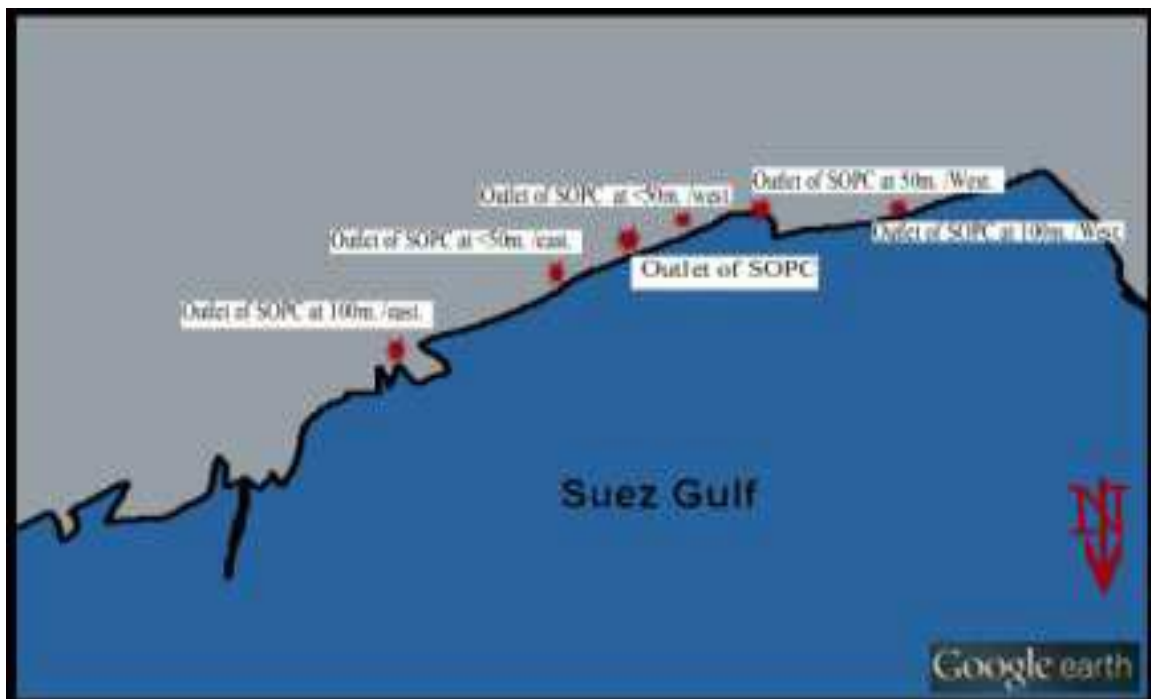
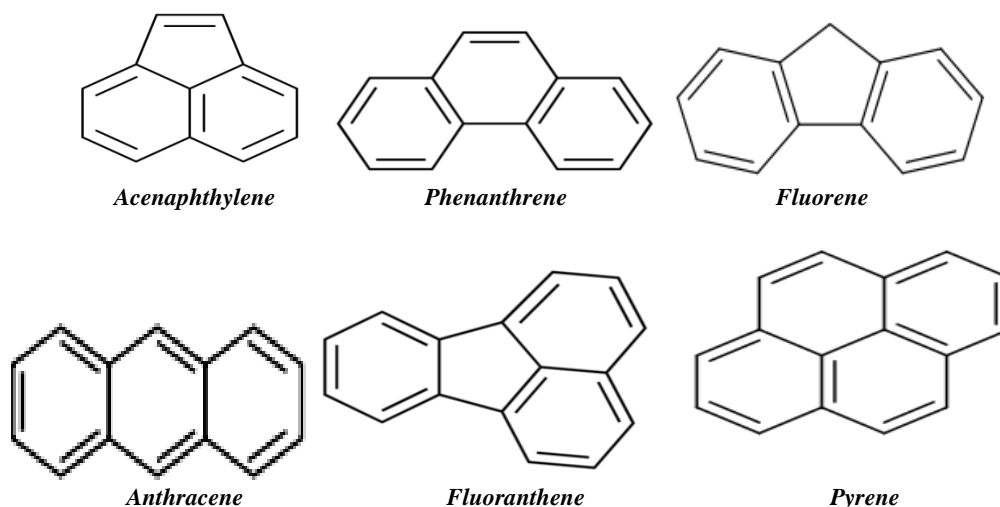


Figure 7: Map of stations along the drainage basin of Suez Oil Petroleum Company (SOPC)



*Figure 8: Chemical structure of the PAHs*

*Table2: The concentration of PAHs in the sample.*

| PAHs                       | Concentration, ppm |
|----------------------------|--------------------|
| Acenaphthylene (A)         | 7.8                |
| Phenanthrene (Phe)         | 1.0                |
| Fluorene (F)               | 7.2                |
| Anthracene (Ant)           | 1.8                |
| Fluoranthene (Flu)         | 3.9                |
| pyrene(Py)                 | 10.6               |
| Benzo(a)anthracene (BaA)   | 0.01               |
| Benzo[b] flourancene (BAf) | 0.03               |
| indeno[1,2,3-] pyrene      | 0.01               |

Preliminary experiments were carried out to evaluate the effect of oxidation conditions on the removal of PAHs. The results confirmed that different aeration rates did not have significant effects on the PAHs removal under the normal condition at natural pH. The main role of air in the solution is to give sufficient oxygen in the polluted water. In presence of photocatalyst, as air is bubbled into solution, O<sub>2</sub> can scavenge the photon-produced electrons on the photocatalyst surface and produce super-oxide radicals. Super-oxide radicals are highly reactive species that could oxidize organic compounds adsorbed on the catalyst surface and the degradation process occurs and improves the degradation rate.

To study the adsorption capacity of the prepared samples, dark experiments were carried out for 15 min before illumination. Up to 14.6 ppm and 11.49 ppm of the total PAHs was disappeared using the samples 0.09 and 0.04 wt.% Cu/TiO<sub>2</sub>, respectively. Figure 8a&b represents a comparison of the photodegradation of the identified compounds. Anthracene undergoes fast degradation. It shows complete degradation after 60 min of irradiation using 0.04 wt. % Cu/TiO<sub>2</sub> and reaches 100% degradation after 30 min of irradiation using 0.09 wt. % Cu/TiO<sub>2</sub>. Phenanthrene showed complete mineralization after 120 min of irradiation using 0.09 wt. % Cu/TiO<sub>2</sub> while the concentration of Phenanthrene reaches 0.23 ppm using 0.04 wt. % Cu/TiO<sub>2</sub>. Fluoranthene (Flu) completely degraded after 240 min of irradiation over 0.09 wt. % Cu/TiO<sub>2</sub> while the concentration reaches 1 ppm using 0.04 wt. %



## International Journal of Engineering Researches and Management Studies

Cu/TiO<sub>2</sub>. Pyrene resists mineralization using 0.04 or 0.09 wt. % Cu/TiO<sub>2</sub>. It is difficult to follow the degradation of Benzo(a)anthracene (BaA), Benzo[b] flourancene (BAf) and indeno[1,2,3-] pyrene due to their very low concentrations.

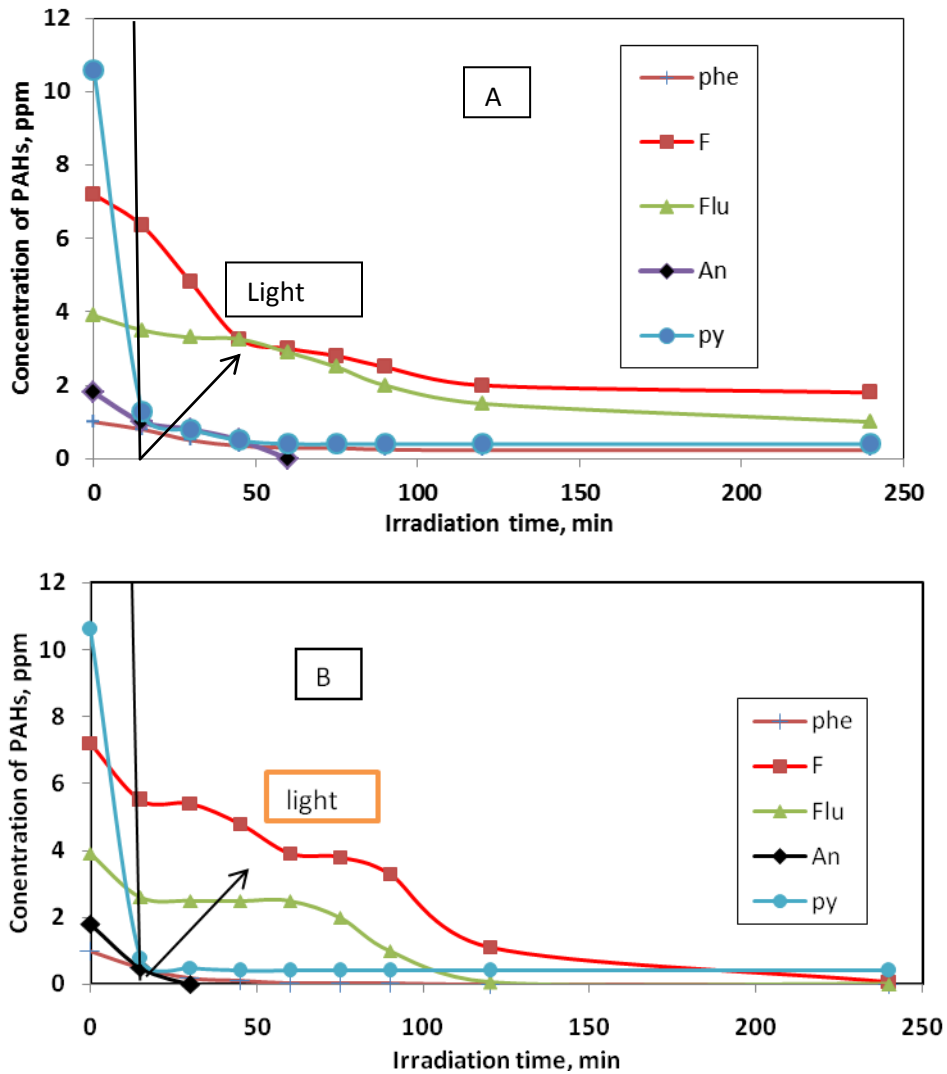


Figure 8: Photocatalytic degradation of PAHs using 0.04wt.% Cu/TiO<sub>2</sub>(A) and 0.09 wt.% Cu/TiO<sub>2</sub>(B) and UV-Vis light.

The photodegradation of the total PAHs displays in Figure 9. It shows that 0.09 wt.% Cu/TiO<sub>2</sub> is more active than 0.04 wt.% Cu/TiO<sub>2</sub>. As the Copper particles loading increases the photocatalytic activity increases. The presence of copper particles on the surface helps to increase the life time of the electron hole pairs by attracting the conduction band photoelectrons. The copper particles on the surface capture the photoelectrons and are subsequently transferred to the adsorbed O<sub>2</sub> to yield highly oxidizing peroxy or superoxy species, leading to the effective separation of electrons and holes and therefore enhance the rate of photocatalytic degradation process.

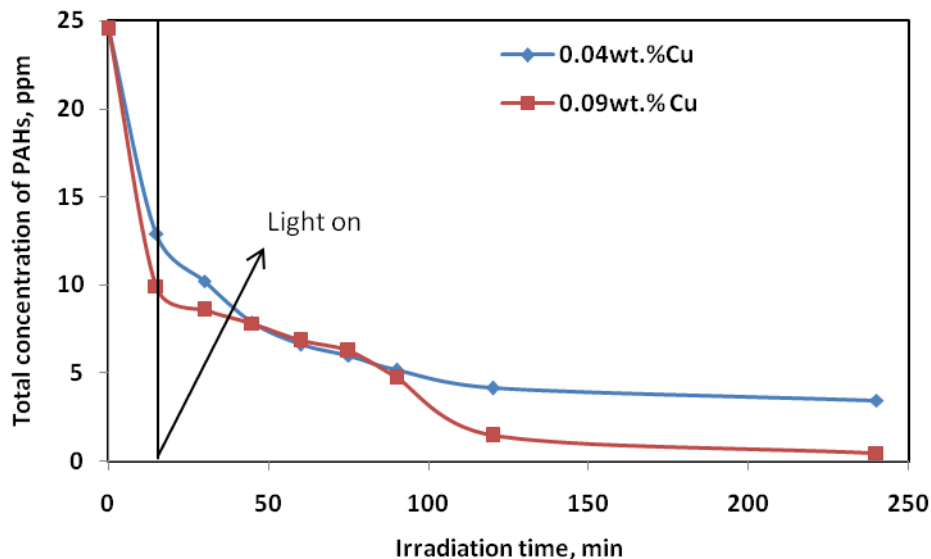


Figure 9: Photocatalytic degradation of total PAHs using 0.04 wt.% Cu/TiO<sub>2</sub> and 0.09 wt.% Cu/TiO<sub>2</sub>.

#### IV. CONCLUSIONS

Different wt.% TiO<sub>2</sub> supported Copper was prepared by wet impregnation method and used as a photocatalyst to remove the PAHs from refinery wastewater. The degradation efficiency of 99% of the organic pollutants was achieved after 240 min of irradiation using 0.09 wt.% Cu/TiO<sub>2</sub> while the degradation reaches 86.4% using 0.04 wt.% Cu/TiO<sub>2</sub>. This result has an industrial impact when this method is considered as an alternative process for biological degradation, having a minimum of 18 h residence time required to provide only 77% removal.

#### V. REFERENCES

1. National Academy of Sciences, 2003, *Oil in the sea III, Inputs, Fates and Effects*.
2. O. E. Ahmed, S. A. Mahmoud, M. M. ElNady, *Egyptian journal of petroleum* <http://dx.doi.org/10.1016/j.ejpe.2016.10.016>
3. I. F. Clement, M.S., Shekoll, and D.G. Shaw, *Macromabathica. Mar. Biol.* 57(1980) 41-50.
4. M. Rebhun, R. Kalabo, L. Grossman, J. Manka, C. Rav-Acha, *Water Res.* 26 (1992) 79-84.
5. S. Demirci, B.R. Erdogan, *Water Res.* 32 (1998) 3495-3499.
6. B. Tensel, J. Regula, *J. Environ. Sci. Health A* 35(2000) 1557-1575.
7. S. Elmaleh, N. Ghaffor, *Water Sci. Technol.* 34 (1996) 231-238.
8. T. Leiknes, M.J. Semmens, *Water Sci. Technol.* 41 (2000) 101-108.
9. S.M. Koh, J.B. Dixon, *Appl. Clay Sci.* 18 (2001) 111-122.
10. Y.A., Sokolov, V.F. Mishukov, V.A. Benerskiy, G.N. Moiseyevski, V.I. Il'ichev, *Dokl. Acad. Sci. USSR, Earth Sci. Sect.* 281(1986) 199-202
11. A.E., Klein, N. Pilpel, *Water Res.* 8(1974) 79-83.
12. N. Daneshvar, M. Rabbani, N. Modirshahla, M.A. Behnajady, *J. Hazard. Mater.* 118 (2005) 155-160.
13. A. Haarstrick, O. Kut, E. Heinzle, *Environ. Sci. Technol.* 30 (1996) 817-824.
14. D.W. Bahnemann, S.N. Kholuiskaya, R. dillert, A.I. Kulak, A.I. Kokorin, *Appl. Catal. B: Environ.* 36 (2002) 161-169.



## International Journal of Engineering Researches and Management Studies

15. J. Chen, M. Liu, L. Zhang, J. Zhang, J. Litong, *Water Res.* 37 (2003) 3815–3820.
16. A. Di Paola, E. Garcia-Lopez, G. Marci, L. Palmisano, *J.Hazard. Mater.* 211 (2012) 3–29.
17. T. Xin, M. Ma, H. Zhang, J. Gu, S. Wang, M. Liu, Q. Zhang, *Appl. Surf. Sci.* 288 (2014) 51–59.
18. R. Asahi, T. Morikawa, T. Ohwaki, K. Aoki, Y. Taga, *Science* 293 (2001) 269–271.
19. K. Woan, G. Pyrgiotakis, W. Sigmund, *Adv. Mater.* 21 (2009) 2233–2239.
20. H. H. El-Maghrabi, E. A. Nada, F. S. Soliman, Y. M. M., A. El-S. Amin, *Egyptian Journal of Petroleum* <http://dx.doi.org/10.1016/j.ejpe.2015.12.004>
21. A. M. Mousa, S. A. Mahmoud and O. E. Ahmed, *Egypt. J. Chem.* 57, 2014, 233 – 255.
22. S.A. Mahmoud, E. Yassitepe, S.I. Shah, *Materials Science Forum* 734 (2013) 215-225.
23. S.J. Gregg, K.S.W. Sing, *Adsorption, Surface Area and Porosity, 2nd ed.*; Academic Press: New York, 1982.
24. H.C. Choi, Y.M. Jung, S.B. Kim, *Vib. Spectrosc.* 37(2005), 33–38.
25. C.C. Yang, S. Li, *J. Phys. Chem. B* 112( 2008) 14193–14197.